Biochimie 220 (2024) 167–178

Contents lists available at ScienceDirect

Biochimie

journal homepage: www.elsevier.com/locate/biochi

Purification and characterization of Cdr1, the drug-efflux pump conferring azole resistance in *Candida* species

Jorgaq Pata [a], Alexis Moreno [a, b], Benjamin Wiseman [c], Sandrine Magnard [a], Idriss Lehlali [a], Marie Dujardin [b], Atanu Banerjee [d], Martin Högbom [c], Ahcène Boumendjel [e], Vincent Chaptal [a], Rajendra Prasad [d], Pierre Falson [a, *]

[a] Drug Resistance & Membrane Proteins Group, CNRS-Lyon 1 University Laboratory UMR 5086, IBCP, 69367, CEDEX Lyon 07, France
[b] CALIXAR, 60 Avenue Rockefeller, Lyon, France
[c] Department of Biochemistry and Biophysics, Arrhenius Laboratories for Natural Sciences, Stockholm University, Stockholm, Sweden
[d] Amity Institute of Biotechnology and Amity Institute of Integrative Sciences and Health, Amity University Haryana, Gurgaon, India
[e] Univ. Grenoble Alpes, INSERM, LRB, 38000, Grenoble, France

ARTICLE INFO

Article history:
Received 11 September 2023
Received in revised form
1 December 2023
Accepted 22 December 2023
Available online 27 December 2023

Handling Editor: Dr B Friguet

Keywords:
ABC transporter
Drug resistance
Membrane proteins
Purification
Efflux pumps

ABSTRACT

Candida albicans and *C. glabrata* express exporters of the ATP-binding cassette (ABC) superfamily and address them to their plasma membrane to expel azole antifungals, which cancels out their action and allows the yeast to become multidrug resistant (MDR). In a way to understand this mechanism of defense, we describe the purification and characterization of Cdr1, the membrane ABC exporter mainly responsible for such phenotype in both species. Cdr1 proteins were functionally expressed in the baker yeast, tagged at their C-terminal end with either a His-tag for the *glabrata* version, *cg*Cdr1-His, or a green fluorescent protein (GFP) preceded by a proteolytic cleavage site for the *albicans* version, *ca*Cdr1-P-GFP. A membrane Cdr1-enriched fraction was then prepared to assay several detergents and stabilizers, probing their level of extraction and the ATPase activity of the proteins as a functional marker. Immobilized metal-affinity and size-exclusion chromatographies (IMAC, SEC) were then carried out to isolate homogenous samples. Overall, our data show that although topologically and phylogenetically close, both proteins display quite distinct behaviors during the extraction and purification steps, and qualify *cg*Cdr1 as a good candidate to characterize this type of proteins for developing future inhibitors of their azole antifungal efflux activity.

1. Introduction

Fungi are a constant health threat. More than 300 million humans are regularly infected by those microorganisms, and among them 3 million displays severe candidemia with a mortality rate up to 50 % [1]. Plants and animals are not spared from this type of infection either, leading to significant reduction in agricultural crops [2]. A large part of human infections by fungi is due to the *Candida* species, a widespread and non-pathogenic yeast genus but aggressively opportunistic under immunocompromised conditions of their host. The most severe form of infection is caused by invasion of blood tissue, which is particularly deadly for immunocompromised patients, particularly after surgery, HIV infection, or even more recently, COVID 19 infection [3]. Other *Candida* species involve *glabrata* [4], *tropicalis* [5], *krusei* [6], and more recently *auris* [7].

Five classes of fungicidal and fungistatic drugs have been developed since 70 years to treat fungal infections [8]. These compounds either disrupt membranes or target the biosynthetic pathways of ergosterol, sphingolipids, microtubules, nucleic acids and cell wall [9]. Among them, azole compounds constitute the most widely used class of antifungals. Early developed [8], azoles block CYP51 [10] which, by demethylating lanosterol generates the ergosterol. This cholesterol-like lipid is specific for the yeast and is required for membrane integrity, accounting for 20 % of the lipid content [11]. Success of azoles is attributed to both their yeast-specific target as well as low cost [12]. They are also used in agriculture, accounting for about 25 % of the fungicides market [13]. The other side of the coin, the massive usage of these molecules favors

* Corresponding author.
E-mail addresses: pierre.falson@ibcp.fr, pfalson@me.com (P. Falson).

https://doi.org/10.1016/j.biochi.2023.12.007
0300-9084/

the development of resistance mechanisms. The appearance of strains resistant to their action rapidly followed their usage [14], a phenomenon that may have been accelerated by their combined use in humans, plants and animals [15].

As a long-lasting response to toxicity induced by the use of azoles, fungi alter the primary structure of the targeted enzyme CYP51 [16]. But as a fast and efficient response to drug administration, fungi detoxify their cytoplasm by upregulating the expression of gene encoding for membrane proteins which act as pumps to expel those drugs out of them, thereby reducing the azoles concentration below their effectiveness threshold [17,18]. These pumps belong primarily to the ATP-binding Cassette (ABC) superfamily [19], early identified in yeast by André Goffeau and colleagues [20], and also to the Major Facilitator Superfamily (MFS) [21]. More worrying, certain representatives of these two families manifest a multi-specificity, a property by which they confer resistance not only to the antifungal agent which triggered their overexpression, but also to other azole or non-azole drugs, *i.e.,* with unrelated structures, that may be subsequently administered. This mechanism leads to a pleiotropic drug resistance (PDR) phenotype [22], which is also observed in cancer cells as a multidrug resistance (MDR) phenotype [23]. Combination of alanine scanning and molecular modeling approaches allowed us to shed light on the molecular basis of this poly-specificity in the case of Mdr1 and Cdr1, the two prominent MFS and ABC proteins of *C. albicans* responsible for the resistance to various antifungal agents, notably azoles [24,25].

PDR exporters represent a significant part of ABC transporters in yeast, with e.g. 10 out of 30 proteins in *Saccharomyces cerevisiæ* [20], 9 out of 26 in *C. albicans* [26] and 7 out of 25 in *C. glabrata* [27]. They share a structural organization made on one hand of 2 nucleotide-binding domains (NBDs) that generate 2 nucleotide-binding sites (NBS) when tightly associated during the transport cycle, and on the other hand of two trans-membrane domains (TMDs) to which drugs bind, are translocated from the inner to the outer membrane leaflet, and then expelled outside the cell. NBDs and TMDs are encoded as a single polypeptide in which one NBD precedes a TMD, a topology also found in the human ABCG sub-family according to the HUGO classification [28]. Progresses in 3D-structure knowledge of ABC transporters have more recently allowed to propose a new classification in which PDR exporters now belong to the type V subfamily [29]; see Moreno et al., 2019 [19] for review. Recently, the first cryo-EM structures of the *S. cerevisiæ* representative, Pdr5, has provided a lot of not only original but also critical information about structural shape and details of PDR exporters [30].

PDR exporters also share an intriguing and uncommon feature by which one of their NBS binds but cannot hydrolyses ATP. Mutagenesis approaches initially carried on Pdr5 [31,32] and later on Cdr1 from *C. albicans* [33,34] highlighted the functional role of this non-catalytic NBS in drug efflux, revealing its pivotal role in the long-distance cross-talk between NBSs and TMDs; see Banerjee et al., 2021 [35] for review. Most of these studies were done *in vivo* or by characterizing the wild-type and mutated proteins in enriched membrane fractions. In order to take a step ahead for characterizing these features on the isolated protein, we have evaluated two different purification strategies based on polyHis and green fluorescent protein (GFP) affinity tagged versions of Cdr1 from two different species, *C. albicans* and *C. glabrata*.

2. Methods

2.1. Materials

Bacto-yeast extract and bacto-peptone were purchased from Difco Laboratories, Detroit, MI. Luria Bertani (LB) medium and YPD medium were purchased from Carl Roth Gmbh & Co. Kg (Karlsruhe, Germany). All detergents including diisobutylene/maleic acid copolymer [36] (DIBMA) and Amphipol A8-35 [37] were purchased from Anatrace Inc., Ohio, USA. Dicarboxylate oside detergent 9b [38] (DCOD 9b) was from CALIXAR, Lyon, France. *Trans*-PCC-α-M [39] (PCC) was purchased from Glycon Biochemicals, Luckenwalde, Germany. CyclAPols C6-C2-50 and C8-C0-50 [40] were kindly provided by Dr. Manuela Zoonens (IBPC, Paris). Competent *Escherichia coli* strain BL21(DE3) Gold pLysS, were purchased from ThemoFisher Scientific, Illkirch, France. The pOPINE-GFP nanobody plasmid [41] was purchased from Addgene, Watertown, MA, USA. EDTA-free antiproteases mix was purchased from Roche SAS, Boulogne-Billancourt, France. SM2 Biobeads were from Biorad laboratories (Hercules CA, USA). The HiFliQ Nickel-NTA columns were purchased from Generon, Slough, UK. Superdex 200 column was purchased from CYTIVA Europe Gmbh, Velizy-Villacoublay, France. Amicon®ultra-centrifugal filters were purchased from Merck KGaA, Darmstadt, Germany. Isopropyl -D-1-thiogalactopyranoside (IPTG), oligomycin and FK506 were purchased from Sigma, L'Isle-d'Abeau Chesnes, France. Peptidisc with the primary sequence FAEKFKEAVKDYFAKFWDPAAEKLKEAVKDYFAKLWD [42] was synthesized chemically by GenScript Biotech Corporation, Jiangsu, China.

2.2. Strain

The yeast strain used in this study was the Δura3 version called ADΔ [43] of the *S. cerevisiæ* AD1-8u⁻ strain in which 7 genes coding for the ABC exporters Yor1 ("1"), Snq2 ("2"), Pdr5 ("3"), Pdr10 ("4"), Pdr11 ("5"), Ycf1 ("6"), Pdr15 ("7"), and one transcription factor, Pdr3 ("8") were deleted, rendering the strain hypersensitive to drugs [44]. ADΔ was a gift of Richard Cannon and Edward Lamping.

2.3. Proteins

The pABC3 plasmids coding for *cg*Cdr1 and caCdr1 studied here were a gift of Richard Cannon and Edward Lamping. *cg*Cdr1 corresponds to the sequence referenced as Q6FK23 in the Uniprot protein database, from the *C. glabrata* laboratory strain CBS 138, to which a hexa-histidine tag had been added at the C-terminal end, leading to the *cg*Cdr1-His chimera [43]. *ca*Cdr1 corresponds to the sequence referenced as P43071 in the Uniprot protein database, from the laboratory strain ATCC 32032, to which a GFP had been fused at the C-terminal end, leading to the *ca*Cdr1-P-GFP chimera [43]. Here, we inserted a PreScission Protease cleavage site (LEVLFQ↓GP) coding sequence between Cdr1 and GFP encoding moieties to generate the *ca*Cdr1-P-GFP chimera. The proteolytic cleavage site was introduced by homologous recombination into the ADΔ strain, using the forward and reverse oligonucleotides 5′-tcgacctggaggtgctgttccagggacctg-3′ and 5′-tcgacaggtccctggaacagcacctccagg-3'. Primary sequences of the *cg*Cdr1-His and *ca*Cdr1-P-GFP constructs are displayed in Table 1.

2.4. Microscopy

Yeast strains were screened by growing them to the exponential phase followed by a wash with phosphate buffer saline (PBS, 137 mM NaCl, 2.7 mM KCl, 10 mM Na_2HPO_4, 1.8 mM KH_2PO_4) and observation in a Zeiss LSM 800 confocal microscope equipped with a Plan-Apochromat 63x/1.40 Oil M27 lens, exiting at 493 and looking for fluorescence emission at 513 nm.

2.5. Drug susceptibility assays

Ten milliliters of YPD medium were inoculated with a single colony of control ADΔ yeast or ADΔ[Cdr1] and further incubated for

Table 1
Primary sequences of Cdr1 constructs. Cdr1 proteins of the *ca*Cdr1-P-GFP and *cg*Cdr1-His chimera correspond to the Uniprot database references P43071 and Q6FK23 (part of each sequence underlined). The PreScission protease cleavage site is in bold and the GFP (Uniprot #P42212) is in italics.

>caCdr1-P-GFP.

.....|.....|.....|.....|.....|.....|.....|.....|.....|.....|

MSDSKMSSQDESKLEKAISQDSSSENHSINEYHGFDAHTSENIQNLARTFTHDSFKDDSSAGLLKYLTHMSEVPGVNPYEHEEINNDQLNPDSENFNAKF
WVKNLRKLFESDPEYYKPSKLGIGYRNLRAYGVANDSDYQPTVTNALWKLATEGFRHFQKDDDSRYFDILKSMDAIMRPGELTVVLGRPGAGCSTLLKTI
AVNTYGFHIGKESQITYDGLSPHDIERHYRGDVIYSAETDVHFPHLSVGDTLEFAARLRTPQNRGEGIDRETYAKHMASVYMATYGLSHTRNTNVGNDFV
RGVSGGERKRVSIAEASLSGANIQCWDNATRGLDSATALEFIRALKTSAVILDTTPLIAIYQCSQDAYDLFDKVVVLYEGYQIFFGKATKAKEYFEKMGW
KCPQRQTTADFLTSLTNPAEREPLPGYEDKVPRTAQEFETYWKNSPEYAELTKEIDEYFVECERSNTRETYRESHVAKQSNNTRPASPYTVSFFMQVRYG
VARNFLRMKGDPSIPIFSVFGQLVMGLILSSVFYNLSQTTGSFYYRGAAMFFAVLFNAFSSLLEIMSLFEARPIVEKHKKYALYRPSADALASIISELPV
KLAMSMSFNFVFYFMVNFRRNPGRFFFYWLMCIWCTFVMSHLFRSIGAVSTSISGAMTPATVLLLAMVIYTGFVIPTPSMLGWSRWINYINPVGYVFESL
MVNEFHGREFQCAQYVPSGPGYENISRSNQVCTAVGSVPGNEMVSGTNYLAGAYQYYNSHKWRNLGITIGFAVFFLAIYIALTEFNKGAMQKGEIVLFLK
GSLKKHKRKTAASNKGDIEAGPVAGKLDYQDEAEAVNNEKFTEKGSTGSVDFPENREIFFWRDLTYQVKIKKEDRVILDHVDGWVKPGQITALMGASGAG
KTTLLNCLSERVTTGIITDGERLVNGHALDSSFQRSIGYVQQQDVHLPTSTVREALQFSAYLRQSNKISKKEKDDYVDYVIDLLEMTDYADALVGVAGEG
LNVEQRKRLTIGVELVAKPKLLLFLDEPTSGLDSQTAWSICKLMRKLADHGQAILCTIHQPSALIMAEFDRLLFLQKGGRTAYFGELGENCQTMINYFEK
YGADPCPKEANPAEWMLQVVGAAPGSHAKQDYFEVWRNSSEYQAVREEINRMEAELSKLPRDNDPEALLKYAAPLWKQYLLVSWRTIVQDWRSPGYIYSK
IFLVVSAALFNGFSFFKAKNNMQGLQNQMFSVFMFFIPFNTLVQQMLPYFVKQRDVYEVREAPSRTFSWFAFIAGQITSEIPYQVAVGTIAFFCWYYPLG
LYNNATPTDSVNPRGVLMWMLVTAFYVYTATMGQLCMSFSELADNAANLATLLFTMCLNFCGVLAGPDVLPGFWIFMYRCNPFTYLVQAMLSTGLANTFV
KCAEREYVSVKPPNGESCSTYLDPYIKFAGGYFETRNDGSCAFCQMSSTNTFLKSVNSLYSERWRNFGIFIAFIAINIILTVIFYWLARVPKGNREKKNK
KVLEVLFQ↓GP*DMSKGEELFTGVVPILVELDGDVNGHKFSVSGEGEGDATYGKLTLKFICTTGKLPVPWPTLVTTFAYGLQCFARYPDHMKRHDFFKSAM
PEGYVQERTIFFKDDGNYKTRAEVKFEGDTLVNRIELKGIDFKEDGNILGHKLEYNYNSHNVYIMADKQKNGIKVNFKIRHNIEDGSVQLADHYQQNTPI
GDGPVLLPDNHYLSTQSALSKDPNEKRDHMVLLEFVTAAGITHGMD

>cgCdr1-His

.....|.....|.....|.....|.....|.....|.....|.....|.....|.....|

MSLASDKKDADVASTTTTAQDDDNLSTYHGFDHHVQDQVRQLARTLTQQSSLHQKKEHTLPEEGINPIFTNTEADDYNPRLDPTSDEFSSAEWVQNMSNI
SNSDPDYYKPYSLGCYWKDLVATGESADIEYQANFLNGPYKGLKTVYNTVVPSTASSKDKNFKILKSMEGAVNPGELLVVLGRPGSGCTTLLKSISSNTH
GFNIAKESTISYSGMTPNDIRKHFRGEVVYNAEADIHLPHLTVYQTLLTVARLKTPQNRLKGIDRETYARHLTEVAMATFGLSHTRNTKVGNDLVRGVSG
GERKRVSIAEVSICGSKFQCWDNATRGLDSATALEFIRALKVQASISNAAATVAIYQCSQDAYDLFDKVCVLYDGYQIYFGPAGKAKEYFQKMGYVSPER
QTTADFLTAVTSPSERIINQDYINRGIFVPQTPKEMWEYWRASEDHADLIKEIDSKLSDNYDANLAEIKDAHVARQSKRARPSSPYTVSYGMQIKYLLIR
NFWRIKQSSGVTLFMVIGNSSMAFILGSMFYKVMKHNTTSTFYFRGAAMFFAVLFNAFSSLLEIFSLFEARPITEKHRTYSLYHPSADAFASILSEVPAK
LITAVCFNIIYYFLVNFRRNGGVFFFYFLINIVAVFAMSHLFRCVGSVSKTLSAAMVPASMLLLGLSMYSGFAIPRTKILGWSKWIWYINPLAYLFESLM
INEFHDRKFPCSQYIPSGSVYNNVPADSRICSSVGAIRGNDYVLGDDFLRESYSYLHKHKWRGFGIGLAYVIFFLVLYLILCEYNEGAKQKGEILVFPQN
IVRRMKKERKLKNVSSDNDVEIGDVSDISDKKILADSSDESEESGANIGLSQSEAIFHWRNLCYDVQIKKETRRILNNVDGWVKPGTLTALMGASGAGKT
TLLDCLAERVTMGVITGEVSVDGKQRDDSFARSIGYCQQQDLHLKTSTVRESLRFSAYLRQPADVSIEEKNQYVEDVIKILEMEQYADAVVGVPGEGLNV
EQRKRLTIGVELAAKPKLLVFLDEPTSGLDSQTAWSICQLMKKLANHGQAILCTIHQPSAILMQEFDRLLFLQRGGKTVYFGDLGDGCKTMIDYFESHGS
HKCPPDANPAEWMLEVVGAAPGSHANQDYHEVWRNSDEYQKVQEELEWMSNELPKKNTNNSETVHKEFATGVLYQCKLVSLRLFQQYWRSPDYLWSKFFL
TIFNNIFIGFTFFKADRSLQGLQNQMLAVFMFTVIFNPLLQQYLPSFVQQRDLYEARERPSRTFSWKAFIVSQILVEIPWNILAGTVAFVIYYYAIGFYS
NASVAHQLHERGALFWLFSCAFYVYIGSLALFCISFNQVAEAAANMASLMFTLSLSFCGVLVTPNGMPRFWIFMYRVSPLTYLIDGMLSTGVANVAIKCS
NYELLRFSPAANLTCGEYLGPYLQTVKTGYIVDPSATDTCELCPYSHTNDFLSSVSSKYSRRWRNWGIFICYIAFNYIAGIFLYWLARVPKKSGKLAKKG
GRHHHHHH

8 h at 30 °C, 200 rpm. Strains sensitivity to xenobiotics was then determined by inoculating yeasts in a 96-well plate at an initial optical density at 600 nm, OD_{600}, of 0.03 using a SAFAS Xenius spectrophotometer (SAFAS, Monaco), in a total volume of 200 μL YPD containing 1 % (w/v) bacto-yeast extract, 2 % (w/v) bacto-peptone and 2 % (w/v) glucose, in presence of a range of drug concentrations. Drugs being solubilized in DMSO, the final concentration of the later was set to 0.5 %. Wells containing test samples were surrounded by wells filled with water to limit evaporation. The plate was then incubated for 14 h at 30 °C, 600 rpm in humidified atmosphere. Yeast growth was then measured at OD_{600}.

2.6. Large-scale yeast cultures

Fifty milliliters of YPD medium were inoculated with a single colony of control ADΔ yeast or ADΔ[Cdr1] and further incubated for 14 h at 30 °C, 200 rpm. The culture was then used to inoculate a 17-L Chemap fermenter (Fermentec, Lyon, France) of YPD medium at an initial OD_{600} of 0.005. Yeasts were grown 14 h at 30 °C, 200 rpm and 2 L air/min. Nitrogen source was refreshed when the OD_{600} reached 1.5 by addition of 10 % (v/v) 5xYP mix containing 100 g/L tryptone and 50 g/L yeast extract. Yeasts were harvested at OD_{600} ~4 by pelleting them at 5000×*g* for 15 min, 4 °C using a JLA-9.1000 rotor (Beckman Coulter). They were then washed twice with ice-cold pure H_2O, weighted (~500×*g*) and diluted 1.5x (w/v) in a Suspension Buffer (SB) containing 50 mM Tris-acetate pH 7.5, 1 mM EDTA, 20 % glycerol, 1 mM PMSF, freshly complemented with an aliquot of EDTA-free antiprotease solution (chymostatin, pepstatin, leupeptin, antipain, aprotinin) at a count of one tablet for 50 mL buffer. Yeast samples were frozen in liquid nitrogen and stored at −80 °C.

2.7. Membrane preparation

Membranes were prepared using a protocol recently described for small-scale cultures [45], that we adapted to large-scale production as follows. Yeasts were thawed in cold water and then mechanically broken with a refrigerated CF cell disruptor (Constant systems Ltd.) by applying a pressure of 1.5 kbar and passing the solution through the disruptor one time, with an outlet lysate temperature remaining below 10 °C. Unbroken material were discarded by pelleting it by two centrifugation steps at 3000×*g* 5 min, 4 °C and a last one at 4200×*g*. The supernatant was 4x diluted in SB and then centrifuged at 20,000×*g* 1 h, 4 °C on a JLA 16.250 rotor (Beckmann Coulter). The resulting membrane fraction pellet was suspended in SB at about 10 g/L protein, estimated by BCA [46]. Membranes were frozen in liquid nitrogen and stored at −80 °C.

2.8. anti-GFP nanobody production and purification

A His-tagged anti-GFP nanobody (nanoantiGFP) was produced in the *E. coli* strain BL21(DE3) Gold pLysS and then purified as described by Kubala and colleagues [41]. Ten milliliters of LB medium (25 g/L) added of with 50 μg/mL ampicillin and chloramphenicol were inoculated with 1 colony of transformed bacteria and then incubated overnight at 37 °C 200 rpm. The culture was used to inoculate 1 L LB supplemented with antibiotics as above, and incubated at 37 °C, 160 rpm, until reaching an OD_{600} of 0.5. The culture was cooled down to 20 °C for about 30 min under shaking and 0.5 mM IPTG was added, followed by 20 h incubation at 20 °C, 160 rpm. The bacteria were then harvested by centrifugation at 5000×*g* with a JLA-9.1000 rotor at 4 °C for 15 min. The pellet was suspended in 50 mM HEPES-HCl, pH 8.0, 1 mM EDTA, anti-protease tablet (one tablet/50 mL). Bacteria were mechanically lysed with a refrigerated CF Constant cell disruptor by applying a pressure of 1.5 kbar and passing the solution through the disruptor two times,

with an outlet lysate temperature remaining below 10 °C. The lysate was centrifuged at 10,000×*g* for 10 min at 4 °C using a JLA 16.250 rotor to discard the unbroken material. The supernatant was loaded into a 5-mL HiFliQ Nickel-NTA resin (Generon) connected to an Aktä Prime™ (GE-healthcare®) purification unit, equilibrated with 50 mM HEPES-HCl buffer pH 8.0, 200 mM NaCl and 40 mM imidazole, at a 2 mL/min flow rate. The resin was washed with 10 vol of the same buffer but 60 mM imidazole and the nanoantiGFP was then eluted by increasing again the imidazole concentration to 250 mM. The pool of nanoantiGFP was frozen in N_2 liquid and stored at −80 °C.

2.9. Cdr1 extraction tests

Assays were carried out at a protein concentration of 5 g/L using 1 % (w/v) extractant and 0.1 % additive (DCOD or cholate) when used, both prepared as 10 % solution in SB, for 1 h, 4 °C under gentle agitation. DIBMA and SMA solutions were used at 2.5 %. Solutions were then centrifuged at 100,000×*g* for 1 h, 4 °C, in a MLA80 rotor (Beckman Coulter) to remove the insoluble material, and loaded on a 10 % acrylamide-bis-acrylamide SDSPAGE [47]. Cdr1 proteins were revealed on SDS-PAGE stained with Coomassie blue stain or illuminated at 473 nm to reveal GFP fluorescence at 510 nm using a Typhoon FLA 9500 Fluorescence Imager (GE Healthcare, Illinois, USA). Proteins on gel were quantified using the Fiji software [48].

2.10. Cdr1 purifications

Extraction. Membrane proteins were extracted as above using 1 % (w/v) detergent. The solution was then centrifuged at 100,000×*g* for 1 h, 4 °C, to remove insoluble material and used immediately further chromatographic steps.

Ion-metal affinity chromatography (IMAC). Both proteins were purified by using a 5-mL HiFliQ Nickel-NTA column connected to an Aktä Prime™ purification unit. This was done either directly for *cg*Cdr1-His or *via* the GFP moiety for *ca*Cdr1-P-GFP, by preloading 10 mol of nanoantiGFP, per mol of extracted *ca*Cdr1-P-GFP, estimated by using the GFP fluorescence. The extracted material was loaded to each resin at a flow rate of 1.0 mL/min and then washed with 50 mM HEPES-HCl, pH 7.5, 150 mM NaCl, 70 μM (2 CMC) PCC ± 4 μM DCOD (as indicated in the text), 20 mM imidazole. Cdr1 proteins were then eluted in 2.0 mL fractions by increasing the imidazole concentration in the buffer up to 150 mM.

Size exclusion chromatography (SEC). Each pool (~10 mL) was concentrated to about 500 μL using Amicon®ultra-centrifugal filters with a cutoff of 100 kDa, at 1500×*g*, a speed reduced for preventing detergent over-accumulation as recently set up [49]. Concentrated solutions were then loaded on a Superdex 200 Increase 10/300 GL column with a running buffer containing 50 mM HEPES-HCl, pH 7.5, 100 mM NaCl, and detergent, either 70 μM (2 CMC) PCC ± 4 μM DCOD (as indicated in the text), 1 mM (6 CMC) DDM or 50 μM (5 CMC) LMNG. Fractions of 1 mL were collected, and the proteins were used immediately or frozen in liquid nitrogen and stored at −80 °C.

PCC – amphipol A8-35 exchange. Fifty-five microliters of an amphipol A8-35 10 % solution in water was mixed with 500 μL of Cdr1 protein solution at 0.6 mg/mL in 50 mM HEPES-HCl, pH 7.5, 150 mM NaCl, 70 μM (2 CMC) PCC, corresponding to an amphipol – protein weight ratio of 10, and incubated for 30 min at room temperature. Then, 20 mg of SM2 Bio-beads, activated as described by the provider, were added to the mixture which was incubated overnight at room temperature. The mixture was then loaded on a Superdex 200 Increase 10/300 GL column equilibrated with 50 mM Tris HCl pH 7.5, 100 mM NaCl.

2.11. Substrate, inhibitors and ligands binding assays

Substrate-binding assays were performed using intrinsic fluorescence, probed on a SAFAS Xenius spectrophotofluorimeter. Tryptophan residues, and N-acetyl tryptophan amide (NATA) used as negative control, were excited at 290 nm with a slot of 5 nm and their fluorescence emission spectra were recorded between 310 and 380 nm with a slot of 5 nm. Experiments were done in a final volume of 200 μL in a quartz cuvette, in which increasing amounts of compounds were added. Resulting emission curves were integrated by summing the fluorescence values between 310 and 380 nm, and deduced from the same experiments carried out with NATA. Alternatively, the binding of Hœchst 33342 was probed by fluorescence resonance energy transfer (FRET), exiting tryptophan residues at 290 nm and recording the emission fluorescence between 400 and 500 nm, corrected from non-specific effects by subtracting the buffer fluorescence. The results were fitted using GraphPad Prism 9 or SigmaPlot V12.5.

2.12. Nano differential scanning fluorimetry (nanoDSF)

Melting temperature (Tm) of each purified protein with and without ligands was determined using a Prometheus NT.48 (NanoTemper Technologies GmbH, München, Germany). Measures were carried out using Cdr1 proteins at 0.2 g/L and a temperature gradient ranging from 20 to 95 °C with a slope of 1 °C/min. Ligands were added at 5 μM for substrates, dyes and inhibitors, 2 mM for ATP-Mg^{2+}-VO_4 and 0.1 μg for yeast lipids (10 % ergosterol content) per μg of Cdr1. Solutions were incubated either for 30 min at room temperature or overnight at 4 °C when containing lipids before measure.

2.13. ATPase activity

ATP hydrolysis in presence of inhibitors and substrates was assayed by measuring the Pi produced for purified protein, in presence and absence of orthovanadate (VO_4) [50]. Alternatively, an ATP regenerating system [51] was also used as follows: reactions were performed at 30 °C in a final volume of 200 μL consisting of 0.1 g/L lactate dehydrogenase, 1 mM phosphoenolpyruvate, 0.1 g/L pyruvate kinase, 0.6 mM NADH, 2 mM $MgCl_2$ and 10 mM KCl. The solution was added of 5 mM NaN_3, 75 mM KNO_3 and 0.3 mM $(NH4)_6Mo_7O_{24}$ as inhibitors of F1 ATPase, pyrophosphatases and phosphatases [52,53], respectively. The mix was added of 4 μg of protein sample and the kinetics was started by adding 5 mM of neutralized ATP-Mg^{2+} and recorded at 340 nm on a SAFAS Xenius spectrophotometer for 10–30 min Cdr1 was then inhibited by adding 20 μM of oligomycin [50] or FK506 [54,55], recording for 10 min more after addition.

2.14. Mathematical and statistical analyses

Data from drug susceptibility assays of the ADΔ strain were fitted with Sigmaplot V12.5 with a logistic equation, 4 parameters, $f = y_0 + a/(1 + abs(x/x_0)^b)$. Kinetics of ATPase activities were fitted using Michaelis-Menten equation V = *VM* * [S]/(*KM* + [S]). ATP-Mg^{2+} and Hœchst 33342 binding data sets were fitted using the equation $f = ABS((F/F0)_{Cdr1}-(F/F0)_{NATA})$, where F is the fluorescence measured at 330 nm for Cdr1 and 350 nm for NATA the latter being used to correct the measures from inner filter and non-specific effects, and F0 is the fluorescence measured in absence of ligand. Data sets were fitted using the ligand-binding equations f = Bmax * [L]/(*Kd* + [L]) or f = Bmax * [L]^h/(*Kd*^h + [L]^h), where Bmax is the maximal fluorescence quenching value, [L] the ligand concentration, *Kd* the constant affinity and h the Hill parameter. Estimated

parameters are in the form of means ± standard deviation (SD) with *p* value when valid, using 1 to 6 independent experiments.

3. Results and discussion

3.1. Generation of the caCdr1-P-GFP chimera and functionality

The *ca*Cdr1-GFP construct originated from a previous work from the Cannon's group [43], aiming at overexpressing Cdr1 from different species, including *C. albicans*, in a highly drug-sensitive strain of *S. cerevisiæ* strain, ADΔ [43]. As reported, this initial construct produced a protein correctly addressed to the plasma membrane, judging by the fluorescence of the GFP moiety well localized at the cell periphery. The protein was also found fully functional by conferring to the host yeast resistance to saturating concentrations of the antifungal drugs fluconazole (FLC) and itraconazole (ITC) [43].

The GFP moiety is widely used to test localization of proteins in cells [56], but less known, it is also suitable for immunopurification of proteins. This was exemplified by Chen and colleagues who enriched the human cystic fibrosis transmembrane conductor regulator protein (CFTR) with a nanobody directed against the GFP fused at its C-terminal end. The authors also used a PreScission Protease cleavage site inserted between both CFTR and GFP for removing the later after purification [57]. In order to test this strategy with *ca*Cdr1-GFP, we also inserted in between the same proteolytic site, LEVLFQ↓GP, resulting in the chimera *ca*Cdr1-P-GFP displayed in Table 1.

We evaluated the functionality of this new construct as before, by looking firstly at its localization in the host yeast using the GFP fluorescence (Fig. 1A). Most of the fluorescence was found well localized at the plasma membrane as expected, however a small fraction remained trapped inside the cytoplasm probably corresponding to a misfolded or degraded fraction of the protein. We thus looked at the resistance to azole antifungals that the modified chimera should confer, Fig. 1B. As expected, we observed a full protection against saturating concentrations of fluconazole and itraconazole, compared to the empty host strain ADΔ that displayed half-maximal cytotoxic concentrations in the micromolar and nanomolar ranges, respectively. The resistance pattern of the modified *ca*Cdr1-P-GFP chimera was also indistinguishable to that of the yeast expressing the *cg*Cdr1-His construct also assayed here, as reported before [43], suggesting a fully functional expression.

3.2. Membrane preparations

Membranes were prepared using a protocol recently set up [45], that we adapted for a large-scale production. We obtained the best yields of Cdr1 enrichment by passing the yeast suspensions through the cell disruptor only one time set to 1.5 kbar. Such pressure was rather low for breaking yeast but yields always reduced when increasing the pressure or repeating one or two times the breaking step. Membrane preparations from ADΔ, ADΔ [*ca*Cdr1-P-GFP] and ADΔ[*cg*Cdr1-GFP] cultures (Fig. 2) gave comparable yields, and for the latter about the same enrichment in

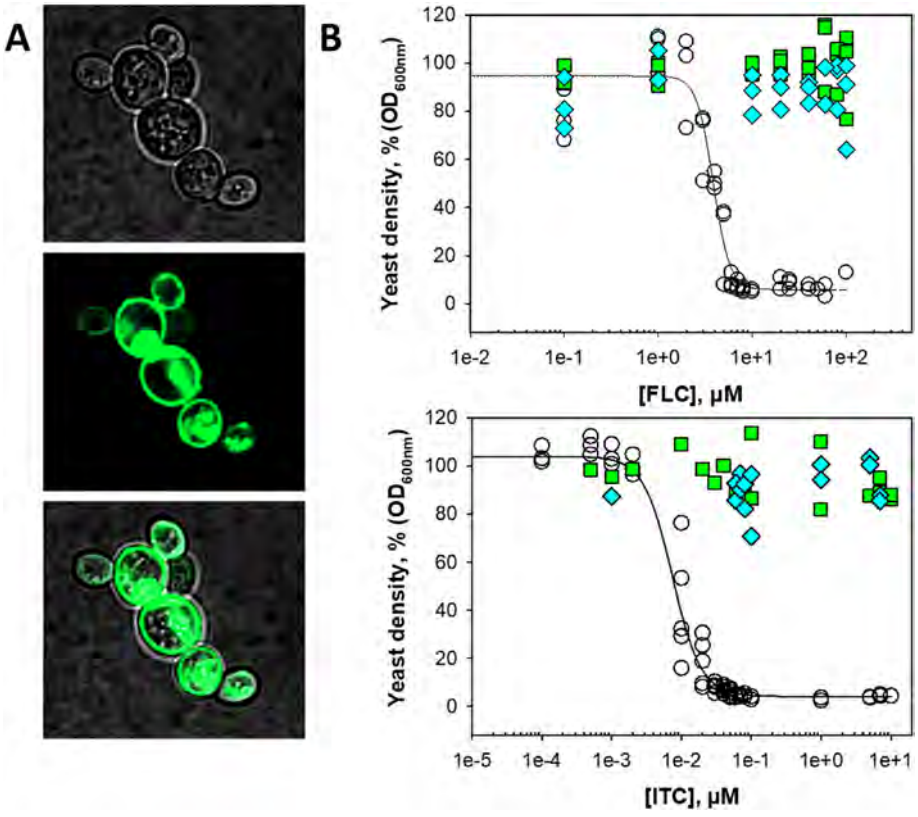

Fig. 1. Functionality of the *ca*Cdr1-P-GFP construct. **A**. Fluorescence of GFP fused to *ca*Cdr1 localization by confocal microscopy. **B**. Resistance and sensitivity pattern to fluconazole (FLC, upper panel) and itraconazole (ITC, lower panel) of ADΔ[*ca*Cdr1-P-GFP] (green squares) compared to the host ADΔ (circles) and ADΔ[*cg*Cdr1-GFP] (blue diamonds) strains. Maximal OD_{600} values obtained in absence of antifungal ranged between 0.9 and 1.2. Half-maximal cytotoxic concentrations, EC_{50}, for the ADΔ strain are of 3.8 ± 0.2 µM and 7.4 ± 0.6 nM ($p < 0.0001$ each) for fluconazole and itraconazole, respectively. **In colors for the print**.

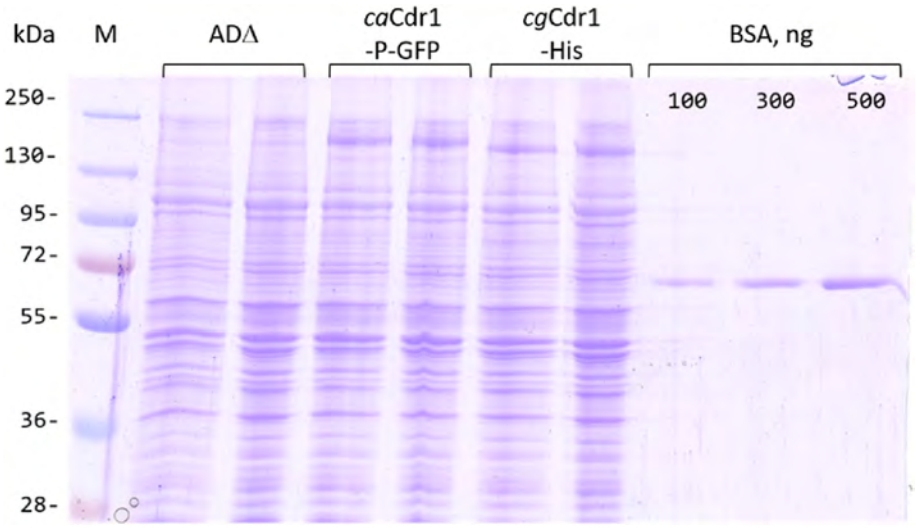

Fig. 2. Yeast membrane fraction preparations and Cdr1 enrichment. Ten micrograms of membrane fraction from ADΔ, ADΔ[*ca*Cdr1-P-GFP] and ADΔ[*cg*Cdr1-GFP] cultures were loaded in duplicate on a 10 % SDS-PAGE, stained after running with Coomassie blue. Indicated amounts of BSA were also loaded for protein content estimation. M: molecular weight markers. **In colors for the print**.

Cdr1of 3.6 ± 0.1 % (w/w, referring to bovine serum albumin, BSA as BCA and Coomassie blue staining standard).

3.3. Cdr1 extraction tests

A series of extractants were assayed to explore Cdr1 solubilization from host membranes. Compounds varied from classical to most recent, used either alone, combined or added to stabilizers. Extractants and stabilizers shown here comprise the dodecyl β-D maltoside (DDM) ± cholate (20 mM DDM, 4.5 mM cholate as described [58]), the undecyl β-D maltoside (UDM), the lauryl maltose neopentyl glycol [59] (LMNG), the foscholine 12 (FC12), the glyco-diosgenin [60] (GDN), the cyclohexyl α-maltoside [39] (PCC) ± dicarboxylate oside 9b [38] (DCOD-9b, 1 mol/20 mol detergent), the polystyrene-co-maleic acid [61] (SMA), the diisobutylene/maleic acid copolymer [36] (DIBMA), and the CyclAPols C6-C2-50 and C8-C0-50 [40]. Extractions tests were mainly assayed with the *ca*Cdr1-P-GFP protein, taking advantage of the GFP moiety easily detectable on SDS-PAGE using a Typhoon imager. Some of them are displayed in Fig. 3A. The protein was extracted 88 % with DDM and in the other conditions between 40 % with SMA and 93 % with FC12. Notably the CyclAPols C6-C2-50 and C8-C0-50 recently developed [40] extracted 78 % of Cdr1. The extraction step had a variable impact on the VO_4-sensitive ATPase activity of the fraction, presumably attributed to Cdr1 by comparing that to the control fraction. No ATPase activity was detected when using SMA, DIBMA co-polymers and CyclAPols. In the case of detergents, the ATPase activity was partially lost to different extents, pointing to LMNG, GDN and PCC for bringing the best results.

The *cg*Cdr1-His protein (panel B) did not display the same extraction patterns with LMNG or GDN, which extracted rather poor amounts of protein although with a good level of ATPase activity, but lower than with the *C. albicans* version. The use of cholate with DDM, which was shown to give a high ATPase activity of the prokaryotic type IV ABC pump BmrA [58], was also of not much use in our case. The protein was extracted pretty well with PCC the but with a very low level of ATPase activity, which was improved when the DCOD-9b was added, the latter having been conceived to stabilize membrane proteins through H-bonds, weak negative charges and hydrophobic interactions [38].

3.4. Metal affinity chromatography step

As introduced above, we used a Nickel-affinity resin to enrich each Cdr1, either indirectly *via* the GFP moiety fused to *ca*Cdr1 bound to a preloaded His-tagged nanoantiGFP or directly *via* the His-tag fused to *cg*Cdr1. Results displayed in Fig. 4 show that both proteins were well enriched and to comparable levels. We expected from the use of the nanoantiGFP to get a better enrichment level as it gives the possibility to remove His-rich contaminants by passing the extracted solution through the resin before loading the nanobody. It turned out that it is not the case, as comparable levels of purity were obtained with both Cdr1 proteins. This is probably due to the imidazole concentration stringency of the conditions used to equilibrate the resin (40 mM imidazole) and wash it after nanobody binding (60 mM imidazole), which strongly limited the contamination. In any case, it remains an excellent strategy to limit the presence of contaminants having a high affinity for the metal.

3.5. Size-exclusion chromatography of Cdr1 proteins

We selected LMNG and PCC as detergents from the extraction tests, compared to the DDM as standard, to evaluate the SEC behavior of *ca*Cdr1-P-GFP. The protein was first enriched by IMAC as described above using either 70 μM PCC, 1 mM DDM or 50 μM LMNG. Each pool of the protein in complex with the nanoantiGFP was then ~10x concentrated and then loaded on a Superdex 200 10/300 column (Fig. 5). Considering the size of such type of protein-detergent complex that we characterized in detail before [62], we expected its elution between 10 and 12 mL, with aggregates eluting in the void volume at about 8 mL. We observed such pattern when using the PCC, with a main peak eluting at 10.2 mL (green trace in panel A). DDM also produced such peak but two additional peaks almost equivalent in size and eluting at 8.5 and 9.2 mL were also present, thus presumably corresponding to oligomeric aggregate of the protein (red trace in panel A). Unexpectedly, LMNG mostly generated only aggregates eluting at the dead volume, suggesting a poor capacity of the detergent to maintain a monomeric state of the complex (blue trace in panel A). PCC exchange with amphipol A8-35 was also assayed, leading to a complex elution profile (black trace in panel A) in which the GFP fluorescence (not shown) allowed to localize the protein mainly under the peak eluting at

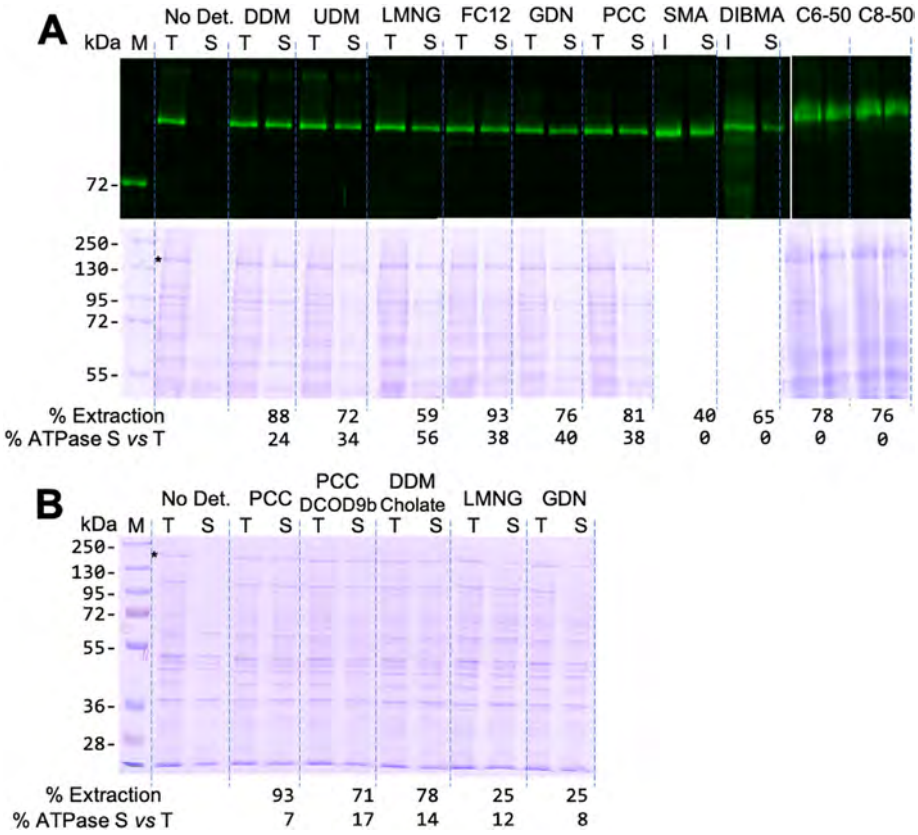

Fig. 3. *ca*Cdr1-P-GFP (A) and *cg*Cdr1-His (B) extraction tests. In-gel fluorescence (**A**, upper panel) and Coomassie blue stained (**A**, lower panel; **B**) gels of 10-μL aliquots of membrane fraction proteins enriched in Cdr1 incubated with each extractant, before (Total) and after (Supernatant) high speed centrifugation. The detergents used for screening were the DDM ± cholate, UDM, LMNG, FC12, GDN, PCC ± DCOD 9b, SMA, DIBMA and CyclAPols C6-C2-50 and C8-C0-50. The Coomassie-blue stained gel is not shown for SMA and DIBMA as they generate a large smear along the lanes. M: molecular weigth markers; *: *ca*Cdr1-P-GFP (**A**) or *cg*Cdr1-His (**B**). The extraction efficacy of Cdr1 was determined by quantifying the GFP fluorescence and/or the Coomassie blue-stained bands on the gels. The ATPase activity corresponds to the vanadate-sensitive fraction measured before and after centrifugation and deduced of that of estimated for the supernatant of the control fraction, typically of about 0.3 μmol/mg Cdr1(gel estimation)/min. Note that the smear generated by DIBMA was not removed by protein precipitation to preserve the functionality of the GFP moiety. **In colors for the print**.

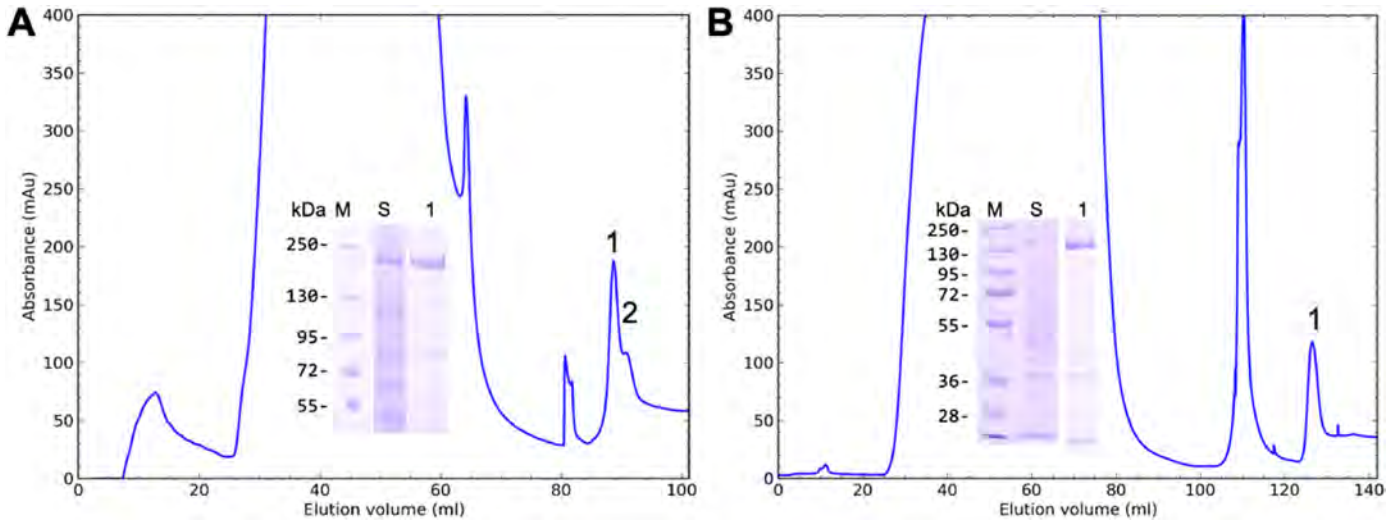

Fig. 4. Metal affinity chromatography of Cdr1 proteins. **A.** IMAC of *ca*Cdr1-P-GFP. Peak 1corresponds to the Cdr1p-P-GFP - nanoantiGFP complex, peak 2 corresponds to the excess of nanoantiGFP. **B.** IMAC of *cg*Cdr1-His. Peak 1corresponds to *cg*Cdr1-His. **In colors for the print**.

10.2 mL. PCC was thus selected and then assayed with *cg*Cdr1-His. A similar profile to that of the *ca*Cdr1-P-GFP-nanoantiGFP complex was obtained, with a main peak eluting slightly later at 10.5 mL due to the difference of molecular mass (dotted trace in panel B). These data confirm that the PCCs prevents, or at least limits, the aggregation tendency of membrane proteins, as also reported previously [63], and seems particularly well adapted to extract and prevent aggregation of yeast ABC pumps, as initially observed with Pdr5

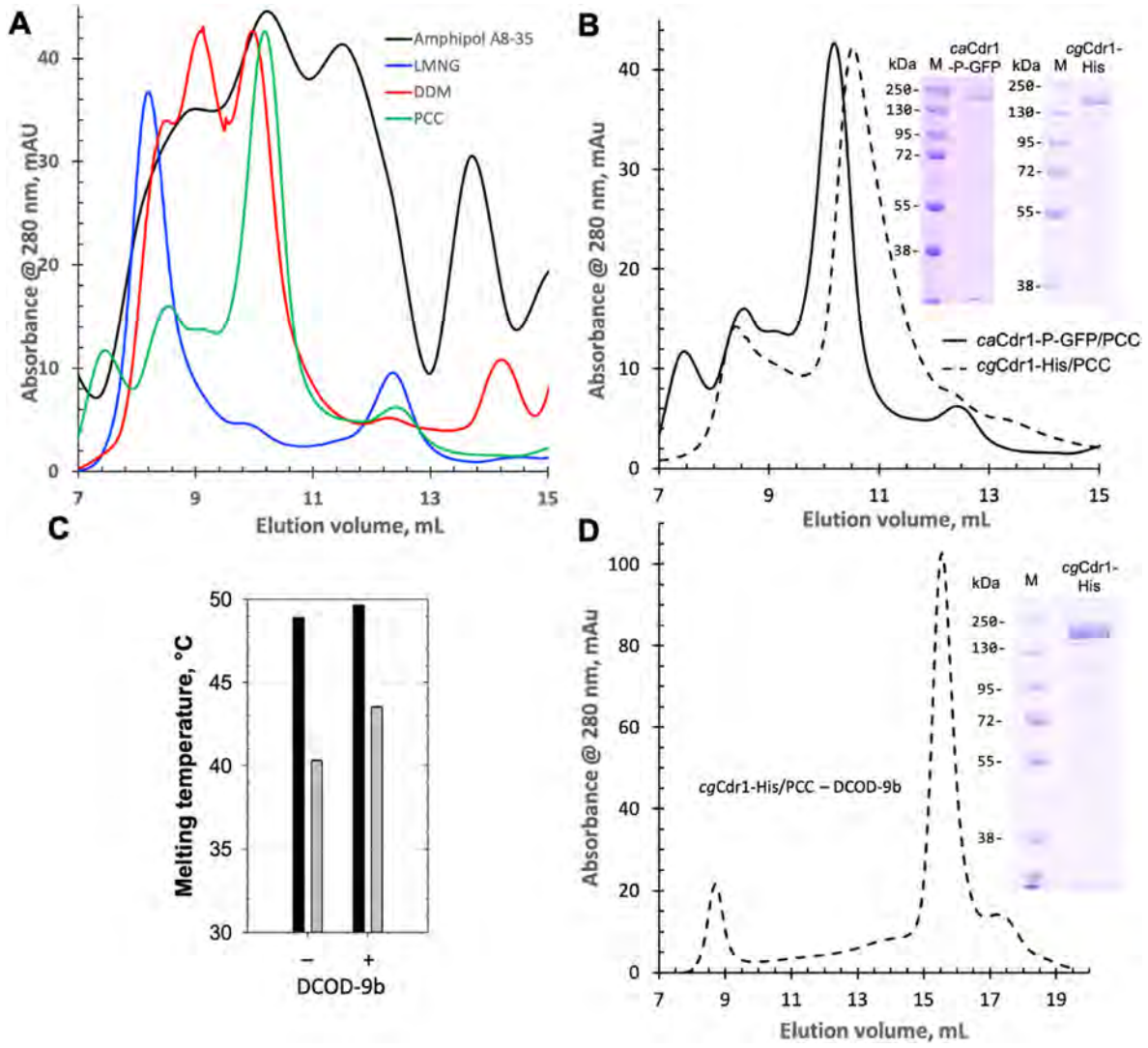

Fig. 5. Size-exclusion chromatography of Cdr1-detergent or amphipol A8-35 complexes. **A**. Superdex 200 10/300 profiles of the *ca*Cdr1-P-GFP-nanoantiGFP complex in solution with either 70 μM PCC (green), 1 mM DDM (red), 50 μM LMNG (blue) or amphipol A8-35 (black). **B**. Superdex 200 10/300 profiles of the *ca*Cdr1-P-GFP-nanoantiGFP complex (solid) and *cg*Cdr1-His (dots) in solution with 70 μM PCC. SDS-PAGE of the head of each main peak. **C**. Melting temperature of the *ca*Cdr1-P-GFP-nanoantiGFP complex (black) and of *cg*Cdr1-His (grey) from panel B with and without 4 μM DCOD-9b, measured by nano-differential scanning fluorimetry. **D.** Superose 200 10/300 profile of *cg*Cdr1-His in solution with 70 μM PCC and 4 μM DCOD-9b. SDS-PAGE of the head of main peak. **In colors for the print**.

from *S. cerevisiæ* [64]. The cyclohexyl tandem forming the alkyl chain of the PCC compared to the aliphatic one of the DDM or the LMNG, and more precisely its higher rigidity as emphasized by its designers [39], seems determining for preserving the membrane region of Cdr1 from exposure to the surrounding water from which originates the aggregation pattern.

Finally, we evaluated the addition of DCOD-9b in the purification process. We previously designed this additive to improve the stability of detergent-extracted membrane proteins by favoring salt-bridge interactions between the 2 carboxylates born by the molecule and the bulk of basic residues enriched at the cytoplasm-membrane interface of the protein. Assayed on BmrA, a prokaryotic ABC pump and A2A, the human adenosine G-protein receptor, both extracted with DDM, the DCOD-9b was found to increase their melting temperature (Tm) by 20 and 10 °C, respectively [38]. Herein, the Cdr1 proteins were firstly purified as above and their Tm was then measured by nano-differential scanning fluorimetry (NanoDSF), which probes the increase of unfolded protein level in respect of the temperature from the intrinsic fluorescence observed at 330 and 350 nm (Fig. 5, panel C). The *ca*Cdr1-P-GFP-nanoantiGFP complex displayed a rather high Tm of ~49 °C, to our surprise much higher than the ~40 °C observed with *cg*Cdr1-His. Addition of DCOD-9b at a 1:20 PCC ratio increased the Tm of *cg*Cdr1-His by ~4 °C, confirming its stabilizing effect. The Tm of the *ca*Cdr1-P-GFP-nanoantiGFP complex was modestly increased by only ~1 °C, maybe due to the high Tm that the protein already displays without additive. In both cases the level of increase in Tm remained lower than that observed initially with BmrA and A2A, which may plausibly be attributed to the higher rigidity of the PCC compared with that of the DDM, as discussed above. We therefore introduced the additive in the purification process at the extraction step and along the chromatographic steps. This is exemplified with the *cg*Cdr1-His protein for which a purification at a preparative scale was then assayed with the additive and which gave a nice SEC profile of a protein eluting quite homogeneously at ~16 mL and lower amount of aggregates eluting at ~8 mL, carried out using a Superose 200 10/300 column (Fig. 5, panel D).

3.6. Biochemical characterization of detergent-purified Cdr1 proteins

As purified, *ca*Cdr1 did not display any ATPase activity (Fig. 6A). Assaying DDM, LMNG, adding or removing DCOD-9b did not change this behavior, nor the addition of lipids, reconstitution of the protein in detergent-free peptidiscs or Amphipol A8-35 environments or removing the GFP tag using the PreScission site (data not shown). On the contrary, *cg*Cdr1 prepared as described displayed an ATPase activity with a *VM* of 0.31 ± 0.06 μmol/min/mg, comparable to that of recently reported for Pdr5 (0.2 μmol/min/mg) [64], but a 3 times poorer *KM* of 1.2 ± 0.7 mM, which is surprisingly rather close to the cytoplasmic ATP concentration (~1.5 mM [65]) (Fig. 6B). Addition of 5 μM fluconazole did neither stimulate or inhibit this activity, hinting at an uncoupling of ATP hydrolysis and substrate transport, and addition of two well-established inhibitors, oligomycin and FK506, inhibited the hydrolysis by 53 % and 64 % respectively (Fig. 6A).

We then evaluated the extent of inactivation of *ca*Cdr1. We took advantage of its ATPase-inactive state to estimate the binding constant of the ATP-Mg^{2+} complex by recording the intrinsic fluorescence of the protein. Indeed, caCdr1 and cgCdr1 have respectively 24 and 25 Trp residues of which, according to the AlphaFold models, 11 are in the NBDs and the rest in the TMDs. The fluorescence quenching remained rather low, caping at 15–20 %, but from which we could estimate a single *Kd* of 134 ± 32 μM ($p = 0.0002$), thus displaying a rather good affinity for the catalytic and non-catalytic ATP-binding sites which looked indistinguishable (Fig. 6C). We then assayed the affinity for transported substrate using the same approach. Adding increasing concentrations of the dye Hœchst 33342 led to a larger fluorescence quenching than observed with nucleotides, caping this time at 40–60 % which is coherent with a fluorescence transfer energy between tryptophan residues and the dye, which is excited at 350 nm. Fitting of the data set allowed to estimate a binding-affinity constant of 1.18 ± 0.09 μM ($p < 0.0001$), close to that of *cg*Cdr1, 0.97 ± 0.05 μM ($p < 0.0001$) assayed in the same conditions, and both rather good considering the detergent environment (Fig. 6D). Same range of values was also measured by FRET (inset panel D). Interestingly, when we carried out the same experiment in the presence of a saturating concentration of ATP-Mg^{2+}, the nucleotide decreased the affinity of the dye to 3.6 ± 0.2 μM ($p < 0.0001$) and triggered an allosteric binding mechanism ($h = 1.33 \pm 0.24$, $p < 0.0001$). This behavior reveals the presence of 2 binding sites for the dye that become distinguishable in a tight ATP-bound state. This observation is in line with the allosteric behavior we previously observed with the human P-glycoprotein transporting the same dye in the presence of the QZSSS inhibitor, which also revealed the presence of 2 Hœchst 33342-binding sites [66]. Overall, these data show that although unable to hydrolyze ATP for a reason remaining to discover, *ca*Cdr1 displays functional substrate binding and inter-domain communication.

3.7. Interaction of Cdr1 proteins with ligands

We then probed the behavior of Cdr1 proteins with various ligands including lipids, azole and non-azole antifungals, dyes (excluding Hœchst 33342 that cannot be used due to its fluorescence parameters), nucleotides and substrate-transport inhibitors by nanoDSF (Fig. 7). Unexpectedly, except for the addition of lipids which reduced the Tm of *ca*Cdr1 by almost 10 °C, none of the other ligands assayed increased or decreased it.

Assayed in the same conditions, *cg*Cdr1 displayed a rather differential levels of stabilization, depending on the ligands. Lipids had no effect, contrarily to what we observed with *ca*Cdr1. Transported substrates such as fluconazole, miconazole, cycloheximide and dyes had either no or poor effect on the Tm. On the contrary, itraconazole triggered an increase of 5 °C. This stabilizing effect may be attributed to the structure of the latter, which is by far the largest one and the most hydrophobic compound of the series assayed here, displaying a Log p of 7.31 *vs* e.g., 0.5 for fluconazole, which probably favors contacts inside the drug-binding pocket.

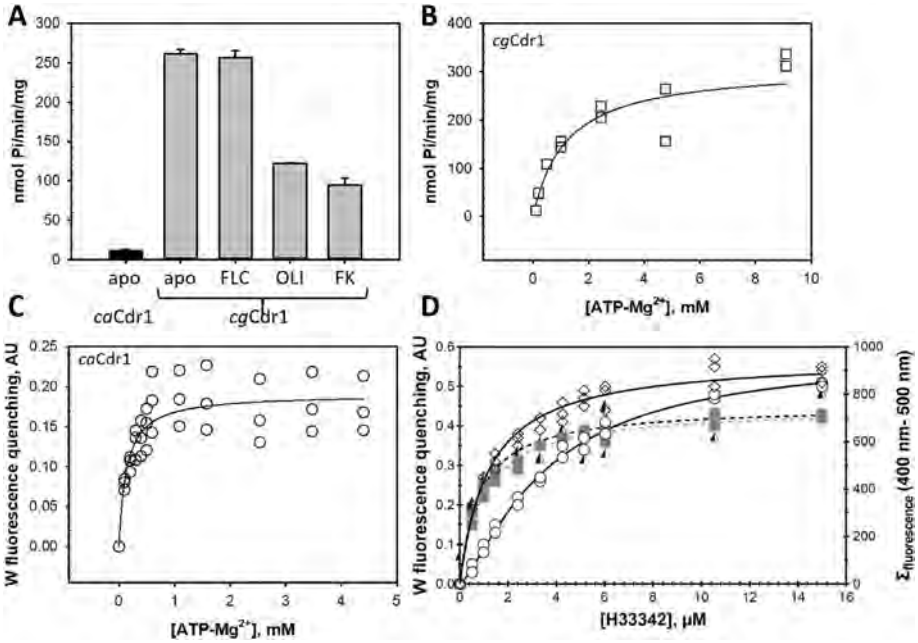

Fig. 6. Biochemical characterization of Cdr1 proteins. A. ATPase activity of detergent-purified Cdr1 without (apo) or with 5 μM substrate (fluconazole, FLC), or inhibitors (oligomycin, OLI, and FK506, FK). **B.** ATPase activity of *cg*Cdr1 as a function of [ATP-Mg^{2+}]. ATPase activities in panels A and B were measured by the release of Pi after 30 min incubation at 37 °C. **C.** ATP-Mg^{2+} binding on *ca*Cdr1 probed by intrinsic fluorescence quenching. **D.** Hœchst 33342 binding probed by intrinsic fluorescence quenching of *cg*Cdr1 (grey squares), and of *ca*Cdr1 in the presence (diamonds) or absence (circles) of 5 mM ATP-Mg^{2+}. Hœchst 33342 binding on *Cg*Cdr1 is also showed, probed by FRET (triangles).

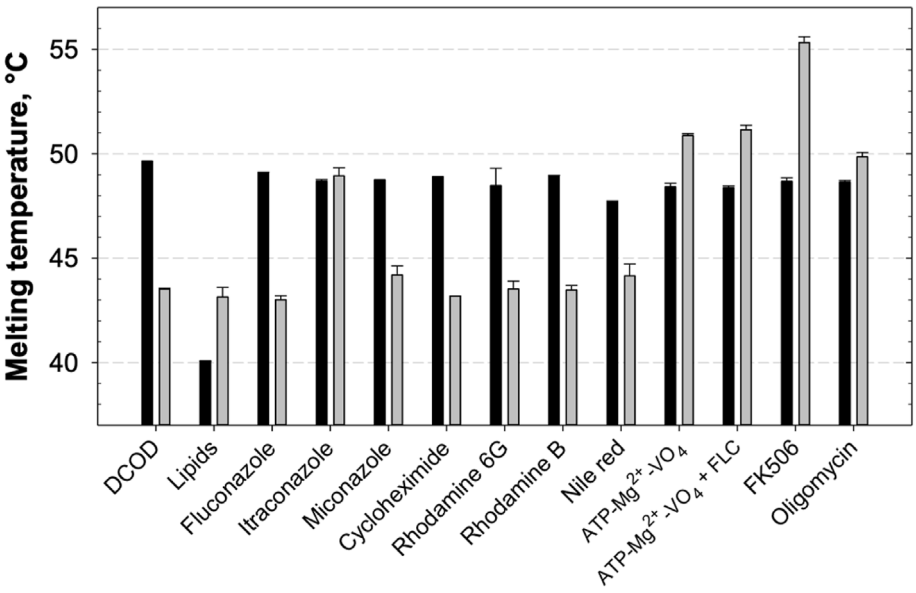

Fig. 7. Melting temperature of Cdr1 proteins with and without ligands measured by nano-differential scanning fluorimetry. Antifungals, dyes and inhibitors were at 5 μM, nucleotides were at 2 mM, yeast lipids (including 10 % ergosterol) were at 0.1 g/g Cdr1.

Addition of ATP-Mg^{2+} and VO_4 which, once hydrolyzed generates an ADP-Mg^{2+}-Pi-VO_4 complex stably bound to the catalytic nucleotide binding site and switches the protein to its outward-facing conformation, had also a significant stabilizing effect on *cg*Cdr1 with a Tm increase of about 7.5 °C. Such an increase was not modulated by the addition of fluconazole. Finally, addition of inhibitors of Cdr1, FK506 and oligomycin, also induced a large increase of the Tm, up to 55 °C in case of FK506, again in contrast to *ca*Cdr1 which did not display any change in the presence of those compounds or with nucleotides.

These data highlighted once again the differences between two proteins. It is likely that *ca*Cdr1 is in a very stable conformation, only modulable by lipids which lower its stability to the same level as *cg*Cdr1. As for *cg*Cdr1, these measures proved that binding of substrates except itraconazole has a small stabilizing effect on the protein, whereas inhibitors are far more efficient. This may be interesting when screening for new inhibitory molecules and may be implemented in a high-throughput screening pipeline.

4. Concluding remarks

In the present study, we set up the purification and characterization of Cdr1 from 2 *Candida* species, *C. albicans* and *C. glabrata* to find conditions in which the protein remains functional in detergent solution. Although the proteins share 70 % identity and confer to their host *S. cerevisiæ* strain a full drug-resistance phenotype to antifungals, assessing their functional overexpression, only Cdr1 from *C. glabrata* remains ATPase-active after the purification process. Cdr1 from *C. albicans* binds drugs and nucleotides but cannot hydrolyze ATP. The extraction and purification steps seem to inactivate the protein suggesting that either specific requirements remain to be discovered and/or progresses remain to be made in detergent, polymers and stabilizers design. In this regard, *ca*Cdr1 seems to be a good tool to develop such new compounds. Meanwhile, *cg*Cdr1 serves as an exciting model to progress the functional and structural characterization and modulation of PDR pumps of pathogenic fungi.

Author contributions

JP and PF conceived the experiments and wrote the Ms; JP, SM, AM, IL, BW and MD did the experiments, ABa, MH, ABo, VC and RP contribute to the writing of the Ms and discussions; PF managed the overall project.

Funding

This work was supported by the Centre National de la Recherche Scientifique (CNRS), Lyon-1 University, Grenoble-Alpes University, the French Research Agency (CLAMP2 - 18-CE11-0002-01 to P.F., A.B. V.C. and S.M.) and the Auvergne-Rhône-Alpes (ARA) region (R&D BOOSTER 2021 – IMABGEN to P.F., V.C., S.M. and M.D.). A.M.'s Ph. D. was supported by grant n° 16 013104 01 ARC SANTE 2016; J.P.'s Ph. D and Master were supported by the doctoral school EDISS and R&D BOOSTER – IMABGEN grants.

Conflicts of interest/disclaimer

Authors declare no conflict of interest.

Declaration of competing interest

The authors declare that they have no known competing financial interests or personal relationships that could have appeared to influence the work reported in this paper.

Acknowledgments

We thank Drs Richard Canon and Edward Lamping for the gift of the strain and Cdr1 expression plasmids.

References

[1] J.-Y. Kim, Human fungal pathogens: why should we learn? J. Microbiol. 54 (2016) 145–148.
[2] Stop neglecting fungi, Nat Microbiol 2 (2017) 17120.
[3] M. Hoenigl, D. Seidel, R. Sprute, C. Cunha, M. Oliverio, G.H. Goldman, A.S. Ibrahim, A. Carvalho, COVID-19-associated fungal infections, Nat Microbiol 7 (2022) 1127–1140.

[4] M. Bolotin-Fukuhara, C. Fairhead, *Candida glabrata*: a deadly companion? Yeast 31 (2014) 279–288.
[5] K.Y. Tseng, Y.C. Liao, F.C. Chen, F.J. Chen, H.J. Lo, A predominant genotype of azole-resistant *Candida tropicalis* clinical strains, Lancet Microbe 3 (2022) e646.
[6] A.T. Jamiu, J. Albertyn, O.M. Sebolai, C.H. Pohl, Update on *Candida krusei*, a potential multidrug-resistant pathogen, Med. Mycol. 59 (2021) 14–30.
[7] H. Du, J. Bing, T. Hu, C.L. Ennis, C.J. Nobile, G. Huang, *Candida auris*: epidemiology, biology, antifungal resistance, and virulence, PLoS Pathog. 16 (2020) e1008921.
[8] E. Drouhet, B. Dupont, Evolution of antifungal agents: past, present, and future, Rev. Infect. Dis. 9 (Suppl 1) (1987) S4–S14.
[9] S. Campoy, J.L. Adrio, Antifungals, Biochem. Pharmacol. 133 (2017) 86–96.
[10] B.C. Monk, A.A. Sagatova, P. Hosseini, Y.N. Ruma, R.K. Wilson, M.V. Keniya, Fungal Lanosterol 14alpha-demethylase: a target for next-generation antifungal design, Biochim. Biophys. Acta, Proteins Proteomics 1868 (2020) 140206.
[11] G. van Meer, D.R. Voelker, G.W. Feigenson, Membrane lipids: where they are and how they behave, Nat. Rev. Mol. Cell Biol. 9 (2008) 112–124.
[12] M. Kneale, J.S. Bartholomew, E. Davies, D.W. Denning, Global access to antifungal therapy and its variable cost, J. Antimicrob. Chemother. 71 (2016) 3599–3606.
[13] L.N. Jorgensen, T.M. Heick, Azole use in agriculture, horticulture, and wood preservation - is it indispensable? Front. Cell. Infect. Microbiol. 11 (2021) 730297.
[14] A.H. Fairlamb, N.A. Gow, K.R. Matthews, A.P. Waters, Drug resistance in eukaryotic microorganisms, Nat Microbiol 1 (2016) 16092.
[15] J.F. Meis, A. Chowdhary, J.L. Rhodes, M.C. Fisher, P.E. Verweij, Clinical implications of globally emerging azole resistance in Aspergillus fumigatus, Philos. Trans. R. Soc. Lond. B Biol. Sci. 371 (2016).
[16] J.E. Parker, A.G. Warrilow, C.L. Price, J.G. Mullins, D.E. Kelly, S.L. Kelly, Resistance to antifungals that target CYP51, J Chem Biol 7 (2014) 143–161.
[17] R.D. Cannon, F.J. Fischer, K. Niimi, M. Niimi, M. Arisawa, Drug pumping mechanisms in *Candida albicans*, Nippon Ishinkin Gakkai Zasshi 39 (1998) 73–78.
[18] R. Prasad, K. Kapoor, Multidrug resistance in yeast *Candida*, Int. Rev. Cytol. 242 (2005) 215–248.
[19] A. Moreno, A. Banerjee, R. Prasad, P. Falson, PDR-like ABC systems in pathogenic fungi, Res. Microbiol. 170 (2019) 417–425.
[20] A. Decottignies, A. Goffeau, Complete inventory of the yeast ABC proteins, Nat. Genet. 15 (1997) 137–145.
[21] M.H. Saier Jr., J.T. Beatty, A. Goffeau, K.T. Harley, W.H. Heijne, S.C. Huang, D.L. Jack, P.S. Jahn, K. Lew, J. Liu, S.S. Pao, I.T. Paulsen, T.T. Tseng, P.S. Virk, The major facilitator superfamily, J. Mol. Microbiol. Biotechnol. 1 (1999) 257–279.
[22] E. Balzi, A. Goffeau, Multiple or pleiotropic drug resistance in yeast, Biochim. Biophys. Acta 1073 (1991) 241–252.
[23] A. Catalano, D. Iacopetta, J. Ceramella, D. Scumaci, F. Giuzio, C. Saturnino, S. Aquaro, C. Rosano, M.S. Sinicropi, Multidrug resistance (MDR): a widespread phenomenon in pharmacological therapies, Molecules 27 (2022).
[24] A. Banerjee, J. Pata, S. Sharma, B.C. Monk, P. Falson, R. Prasad, Directed mutational strategies reveal drug binding and transport by the MDR transporters of *Candida albicans*, J Fungi (Basel) 7 (2021).
[25] A.K. Redhu, A. Banerjee, A.H. Shah, A. Moreno, M.K. Rawal, R. Nair, P. Falson, R. Prasad, Molecular basis of substrate polyspecificity of the *Candida albicans* Mdr1p multidrug/H(+) antiporter, J. Mol. Biol. 430 (2018) 682–694.
[26] M. Gaur, D. Choudhury, R. Prasad, Complete inventory of ABC proteins in human pathogenic yeast, *Candida albicans*, J. Mol. Microbiol. Biotechnol. 9 (2005) 3–15.
[27] S. Kumari, M. Kumar, N.K. Khandelwal, P. Kumari, M. Varma, P. Vishwakarma, G. Shahi, S. Sharma, A.M. Lynn, R. Prasad, N.A. Gaur, ABC transportome inventory of human pathogenic yeast *Candida glabrata*: phylogenetic and expression analysis, PLoS One 13 (2018) e0202993.
[28] S. Povey, R. Lovering, E. Bruford, M. Wright, M. Lush, H. Wain, The HUGO gene nomenclature committee (HGNC), Hum. Genet. 109 (2001) 678–680.
[29] C. Thomas, S.G. Aller, K. Beis, E.P. Carpenter, G. Chang, L. Chen, E. Dassa, M. Dean, F. Duong Van Hoa, D. Ekiert, R. Ford, R. Gaudet, X. Gong, I.B. Holland, Y. Huang, D.K. Kahne, H. Kato, V. Koronakis, C.M. Koth, Y. Lee, O. Lewinson, R. Lill, E. Martinoia, S. Murakami, H.W. Pinkett, B. Poolman, D. Rosenbaum, B. Sarkadi, L. Schmitt, E. Schneider, Y. Shi, S.L. Shyng, D.J. Slotboom, E. Tajkhorshid, D.P. Tieleman, K. Ueda, A. Varadi, P.C. Wen, N. Yan, P. Zhang, H. Zheng, J. Zimmer, R. Tampe, Structural and functional diversity calls for a new classification of ABC transporters, FEBS Lett. 594 (2020) 3767–3775.
[30] A. Harris, M. Wagner, D. Du, S. Raschka, L.M. Nentwig, H. Gohlke, S.H.J. Smits, B.F. Luisi, L. Schmitt, Structure and efflux mechanism of the yeast pleiotropic drug resistance transporter Pdr5, Nat. Commun. 12 (2021) 5254.
[31] Z.E. Sauna, S.S. Bohn, R. Rutledge, M.P. Dougherty, S. Cronin, L. May, D. Xia, S.V. Ambudkar, J. Golin, Mutations define cross-talk between the N-terminal nucleotide-binding domain and transmembrane helix-2 of the yeast multidrug transporter Pdr5: possible conservation of a signaling interface for coupling ATP hydrolysis to drug transport, J. Biol. Chem. 283 (2008) 35010–35022.
[32] M.T. Downes, J. Mehla, N. Ananthaswamy, A. Wakschlag, M. Lamonde, E. Dine, S.V. Ambudkar, J. Golin, The transmission interface of the Saccharomyces cerevisiae multidrug transporter Pdr5: val-656 located in intracellular loop 2 plays a major role in drug resistance, Antimicrob. Agents Chemother. 57 (2013) 1025–1034.
[33] A. Banerjee, A. Moreno, M.F. Khan, R. Nair, S. Sharma, S. Sen, A.K. Mondal, J. Pata, C. Orelle, P. Falson, R. Prasad, Cdr1p highlights the role of the non-hydrolytic ATP-binding site in driving drug translocation in asymmetric ABC pumps, Biochim. Biophys. Acta Biomembr. 1862 (2020) 183131.
[34] A. Banerjee, A.H. Shah, A.K. Redhu, A. Moreno, P. Falson, R. Prasad, W1038 near D-loop of NBD2 is a focal point for inter-domain communication in multidrug transporter Cdr1 of *Candida albicans*, Biochim. Biophys. Acta Biomembr. 1860 (2018) 965–972.
[35] A. Banerjee, A. Moreno, J. Pata, P. Falson, R. Prasad, ABCG: a new fold of ABC exporters and a whole new bag of riddles, Adv Protein Chem Struct Biol 123 (2021) 163–191.
[36] A.O. Oluwole, B. Danielczak, A. Meister, J.O. Babalola, C. Vargas, S. Keller, Solubilization of membrane proteins into functional lipid-bilayer nanodiscs using a diisobutylene/maleic acid copolymer, Angew Chem. Int. Ed. Engl. 56 (2017) 1919–1924.
[37] C. Tribet, R. Audebert, J.L. Popot, Amphipols: polymers that keep membrane proteins soluble in aqueous solutions, Proc. Natl. Acad. Sci. U.S.A. 93 (1996) 15047–15050.
[38] K.A. Nguyen, M. Peuchmaur, S. Magnard, R. Haudecoeur, C. Boyere, S. Mounien, I. Benammar, V. Zampieri, S. Igonet, V. Chaptal, A. Jawhari, A. Boumendjel, P. Falson, Glycosyl-substituted dicarboxylates as detergents for the extraction, overstabilization, and crystallization of membrane proteins, Angew Chem. Int. Ed. Engl. 57 (2018) 2948–2952.
[39] J. Hovers, M. Potschies, A. Polidori, B. Pucci, S. Raynal, F. Bonnete, M.J. Serrano-Vega, C.G. Tate, D. Picot, Y. Pierre, J.L. Popot, R. Nehme, M. Bidet, I. Mus-Veteau, H. Busskamp, K.H. Jung, A. Marx, P.A. Timmins, W. Welte, A class of mild surfactants that keep integral membrane proteins water-soluble for functional studies and crystallization, Mol. Membr. Biol. 28 (2011) 171–181.
[40] A. Marconnet, B. Michon, C. Le Bon, F. Giusti, C. Tribet, M. Zoonens, Solubilization and stabilization of membrane proteins by cycloalkane-modified amphiphilic polymers, Biomacromolecules 21 (2020) 3459–3467.
[41] M.H. Kubala, O. Kovtun, K. Alexandrov, B.M. Collins, Structural and thermodynamic analysis of the GFP:GFP-nanobody complex, Protein Sci. 19 (2010) 2389–2401.
[42] M.L. Carlson, J.W. Young, Z. Zhao, L. Fabre, D. Jun, J. Li, J. Li, H.S. Dhupar, I. Wason, A.T. Mills, J.T. Beatty, J.S. Klassen, I. Rouiller, F. Duong, The Peptidisc, a simple method for stabilizing membrane proteins in detergent-free solution, Elife 7 (2018).
[43] E. Lamping, B.C. Monk, K. Niimi, A.R. Holmes, S. Tsao, K. Tanabe, M. Niimi, Y. Uehara, R.D. Cannon, Characterization of three classes of membrane proteins involved in fungal azole resistance by functional hyperexpression in *Saccharomyces cerevisiae*, Eukaryot. Cell 6 (2007) 1150–1165.
[44] A. Decottignies, A.M. Grant, J.W. Nichols, H. de Wet, D.B. McIntosh, A. Goffeau, ATPase and multidrug transport activities of the overexpressed yeast ABC protein Yor1p, J. Biol. Chem. 273 (1998) 12612–12622.
[45] G. Madani, E. Lamping, H.J. Lee, M. Niimi, A.K. Mitra, R.D. Cannon, Small-scale plasma membrane preparation for the analysis of *Candida albicans* cdr1-mGFPHis, J. Vis. Exp. (2021) 172.
[46] P.K. Smith, R.I. Krohn, G.T. Hermanson, A.K. Mallia, F.H. Gartner, M.D. Provenzano, E.K. Fujimoto, N.M. Goeke, B.J. Olson, D.C. Klenk, Measurement of protein using bicinchoninic acid, Anal. Biochem. 150 (1985) 76–85.
[47] U.K. Laemmli, Cleavage of structural proteins during the assembly of the head of bacteriophage T4, Nature 227 (1970) 680–685.
[48] J. Schindelin, I. Arganda-Carreras, E. Frise, V. Kaynig, M. Longair, T. Pietzsch, S. Preibisch, C. Rueden, S. Saalfeld, B. Schmid, J.Y. Tinevez, D.J. White, V. Hartenstein, K. Eliceiri, P. Tomancak, A. Cardona, Fiji: an open-source platform for biological-image analysis, Nat. Methods 9 (2012) 676–682.
[49] A. Gobet, V. Zampieri, S. Magnard, E. Pebay-Peyroula, P. Falson, V. Chaptal, The non-Newtonian behavior of detergents during concentration is increased by macromolecules, in: Trans, and Results in Their Over-concentration, Biochimie, 2022.
[50] A. Decottignies, M. Kolaczkowski, E. Balzi, A. Goffeau, Solubilization and characterization of the overexpressed PDR5 multidrug resistance nucleotide triphosphatase of yeast, J. Biol. Chem. 269 (1994) 12797–12803.
[51] M.E. Pullman, H.S. Penefsky, A. Datta, E. Racker, Partial resolution of the enzymes catalyzing oxidative phosphorylation. I. Purification and properties of soluble dinitrophenol-stimulated adenosine triphosphatase, J. Biol. Chem. 235 (1960) 3322–3329.
[52] F. Centeno, S. Deschamps, A.M. Lompre, M. Anger, M.J. Moutin, Y. Dupont, M.G. Palmgren, J.M. Villalba, J.V. Moller, P. Falson, et al., Expression of the sarcoplasmic reticulum Ca^{2+}-ATPase in yeast, FEBS Lett. 354 (1994) 117–122.
[53] P. Falson, T. Menguy, F. Corre, L. Bouneau, A.G. de Gracia, S. Soulie, F. Centeno, J.V. Moller, P. Champeil, M. le Maire, The cytoplasmic loop between putative transmembrane segments 6 and 7 in sarcoplasmic reticulum Ca^{2+}-ATPase binds Ca^{2+} and is functionally important, J. Biol. Chem. 272 (1997) 17258–17262.
[54] A. Kralli, K.R. Yamamoto, An FK506-sensitive transporter selectively decreases intracellular levels and potency of steroid hormones, J. Biol. Chem. 271 (1996) 17152–17156.
[55] S. Maesaki, P. Marichal, M.A. Hossain, D. Sanglard, H. Vanden Bossche, S. Kohno, Synergic effects of tactolimus and azole antifungal agents against azole-resistant *Candida albicans* strains, J. Antimicrob. Chemother. 42 (1998) 747–753.
[56] R.Y. Tsien, The green fluorescent protein, Annu. Rev. Biochem. 67 (1998)

509–544.
[57] F. Liu, Z. Zhang, L. Csanady, D.C. Gadsby, J. Chen, Molecular structure of the human CFTR ion channel, Cell 169 (2017) 85–95 e88.
[58] V. Chaptal, V. Zampieri, B. Wiseman, C. Orelle, J. Martin, K.A. Nguyen, A. Gobet, M. Di Cesare, S. Magnard, W. Javed, J. Eid, A. Kilburg, M. Peuchmaur, J. Marcoux, L. Monticelli, M. Hogbom, G. Schoehn, J.M. Jault, A. Boumendjel, P. Falson, Substrate-bound and substrate-free outward-facing structures of a multidrug ABC exporter, Sci. Adv. 8 (2022) eabg9215.
[59] P.S. Chae, S.G. Rasmussen, R.R. Rana, K. Gotfryd, R. Chandra, M.A. Goren, A.C. Kruse, S. Nurva, C.J. Loland, Y. Pierre, D. Drew, J.L. Popot, D. Picot, B.G. Fox, L. Guan, U. Gether, B. Byrne, B. Kobilka, S.H. Gellman, Maltose-neopentyl glycol (MNG) amphiphiles for solubilization, stabilization and crystallization of membrane proteins, Nat. Methods 7 (2010) 1003–1008.
[60] P.S. Chae, S.G. Rasmussen, R.R. Rana, K. Gotfryd, A.C. Kruse, A. Manglik, K.H. Cho, S. Nurva, U. Gether, L. Guan, C.J. Loland, B. Byrne, B.K. Kobilka, S.H. Gellman, A new class of amphiphiles bearing rigid hydrophobic groups for solubilization and stabilization of membrane proteins, Chemistry 18 (2012) 9485–9490.
[61] S. Gulati, M. Jamshad, T.J. Knowles, K.A. Morrison, R. Downing, N. Cant, R. Collins, J.B. Koenderink, R.C. Ford, M. Overduin, I.D. Kerr, T.R. Dafforn, A.J. Rothnie, Detergent-free purification of ABC (ATP-binding-cassette) transporters, Biochem. J. 461 (2014) 269–278.
[62] V. Chaptal, F. Delolme, A. Kilburg, S. Magnard, C. Montigny, M. Picard, C. Prier, L. Monticelli, O. Bornert, M. Agez, S. Ravaud, C. Orelle, R. Wagner, A. Jawhari, I. Broutin, E. Pebay-Peyroula, J.M. Jault, H.R. Kaback, M. le Maire, P. Falson, Quantification of detergents complexed with membrane proteins, Sci. Rep. 7 (2017) 41751.
[63] J.W. Missel, N. Salustros, E.R. Becares, J.H. Steffen, A.G. Laursen, A.S. Garcia, M.M. Garcia-Alai, C. Kolar, P. Gourdon, K. Gotfryd, Cyclohexyl-alpha maltoside as a highly efficient tool for membrane protein studies, Curr Res Struct Biol 3 (2021) 85–94.
[64] M. Wagner, S.H.J. Smits, L. Schmitt, *In vitro* NTPase activity of highly purified Pdr5, a major yeast ABC multidrug transporter, Sci. Rep. 9 (2019) 7761.
[65] H. Osorio, E. Carvalho, M. del Valle, M.A. Gunther Sillero, P. Moradas-Ferreira, A. Sillero, H2O2, but not menadione, provokes a decrease in the ATP and an increase in the inosine levels in *Saccharomyces cerevisiae*. An experimental and theoretical approach, Eur. J. Biochem. 270 (2003) 1578–1589.
[66] L. Martinez, O. Arnaud, E. Henin, H. Tao, V. Chaptal, R. Doshi, T. Andrieu, S. Dussurgey, M. Tod, A. Di Pietro, Q. Zhang, G. Chang, P. Falson, Understanding polyspecificity within the substrate-binding cavity of the human multidrug resistance P-glycoprotein, FEBS J. 281 (2014) 673–682.